5810 *Inorg. Chem.* **2009**, *48*, 5810–5819
DOI: 10.1021/ic900058q

Inorganic Chemistry
Article

# Radical Bonding: Structure and Stability of Bis(Phenalenyl) Complexes of Divalent Metals from across the Periodic Table

**Smaranda Craciun and Kelling J. Donald***

*Department of Chemistry, Gottwald Center for the Sciences, University of Richmond, Richmond, Virginia 23173*

Received January 12, 2009

We examine the bonding possibilities of the bis(phenalenyl) M$P_2$ sandwich complexes of the divalent metals M = Be, Mg, Ca, Sr, Ba, Zn, Cd, and Hg, at the B3LYP level of theory. The outcome is an extraordinarily diverse class of low symmetry bis(phenalenyl)metal complexes in which bonding preferences and binding enthalpies differ dramatically. The lowest energy group 2 metal M$P_2$ complexes include an intriguing $\eta^1$,$\eta^3$ Be$P_2$ structure, and bent $\eta^6$,$\eta^6$ systems for M = Ca, Sr, and Ba. The group 12 bis(phenalenyl) complexes are thermodynamically unstable $\eta^1$,$\eta^1$ slip-sandwich structures. To better understand changes in the structural preferences going from the ($\eta^6$,$\eta^6$) group 2 to the ($\eta^1$,$\eta^1$) group 12 complexes, we explored the bonding in the bis(phenalenyl) complexes of transition metals with stable +2 oxidations states between Ca and Zn in period 4. The computed binding enthalpies are large and negative for nearly all of the minimum energy bis(phenalenyl) complexes of the group 2 and the transition metals; they are tiny for Mg$P_2$, and are quite positive for the group 12 systems. The structural preferences and stability of the complexes is a subtle negotiation of several influences: the (un)availability of ($n$ − 1)d and $n$p, orbitals for bonding, the cost of the rehybridization at carbon sites in the phenalenyl rings in preparation for bonding to the metals, and the ($P$—$P$) interaction between the phenalenyl radicals.

## Introduction

The phenalenyl radical, $P$, is an odd-alternant hydrocarbon with a trigonal planar carbon center surrounded by an antiaromatic 12-carbon ring (Figure 1).[1] An alternative way to talk about this system is as a substituted naphthalene derivative, hence its identification in the early literature as the perinaphthyl radical[1−4] or acenaphthenyl in Coulson and Streitweiser's Dictionary.[5] Various studies during the 1950s and early 1960s established the unusual stability of this free radical (Figure 1),[1−7] and its monoanion and monocation.[1,7]

Even before the radical was detected experimentally,[1,3,4] it was suggested that the high symmetry of the species may allow significant resonance stabilization, with the radical electron delocalized around the external (twelve carbon) ring.[2,8] $P$ is stable in solution over a period of months,[1,3a] and is believed to be present in petroleum and some of its derivatives.[1,3b,9]

In a localized representation, the structure of $P$ is usually drawn with the radical electron located at the central carbon (atom 9b in Figure 1). There are, of course, other resonance structures that place the unpaired electron along the periphery, and electronic calculations at various levels of sophistication agree that the singly occupied molecular orbital (SOMO) has an electron density of zero at the central atom. The SOMO is, in fact, the nonbonding $\mathrm{A}_1''$ molecular orbital depicted in Figure 2a.[1,10]

A pretty orbital. Could its exquisite shape be put to work? To put it another way, what systems (atoms or molecules) have orbitals of the appropriate energy and symmetry to form a bond with $P$ in which some or, at an extreme, all six lobes of the SOMO (Figure 2a) participate?

One known example of a bond between $P$ and another chemical species is the dimer of $P$ itself. The substituted radical, with *tert*-butyls at positions 2, 5, and 8 (in Figure 1),[11] is known to form a $D_{3d}$ face-to-face dimer.[11,12] The dimers of this stable substituted radical are of interest, in part, because the experimentally observed face to face distance of 3.3 Å is

---

*To whom correspondence should be addressed. E-mail: kdonald@richmond.edu.

(1) Reid, D. H. *Quart. Rev. (London)* 274, *19*, **1965**. The preparation and properties of the phenalenyl radical are described in Section 4.4, pp 286−288 of this review.

(2) Boekelheide, V.; Goldman, M. *J. Am. Chem. Soc.* **1954**, *76*, 604.

(3) (a) Sogo, P. B.; Nakazaki, M.; Calvin, M. *J. Chem. Phys.* **1957**, *26*, 1343. (b) Sterling, F. C.; Bartz, K. W. *J. Chem. Phys.* **1961**, *34*, 1076.

(4) Bennett, J. E. *Proc. Chem. Soc.* **1961**, 144.

(5) Coulson, C. A.; Streitweiser, A. *Dictionary of π-electron Calculations*; Oxford: Pergamon, 1965.

(6) Gold, V.; Tye, F. L. *J. Chem. Soc.* **1952**, 2184.

(7) Pettit, R. *J. Am. Chem. Soc.* **1960**, *82*, 1972.

(8) Boekelheide, V; Larrabee, C. E. *J. Am. Chem. Soc.* **1950**, *72*, 1245.

(9) Corio, P. L. *Chem. Rev.* **1960**, *60*, 363, and references therein.

(10) Haddon, R. C. *Aust. J. Chem.* **1975**, *28*, 2343.

(11) Goto, K.; Kubo, T.; Yamamoto, K.; Nakasuji, K.; Sato, K.; Shiomi, D.; Takui, T.; Kubota, M.; Kobayashi, T.; Yakusi, K.; Ouyang, J. *J. Am. Chem. Soc.* **1999**, *121*, 1619.

(12) Fukui, K.; Sato, K.; Shiomi, D.; Takui, T.; Itoh, K.; Goto, K.; Kubo, T.; Yamamoto, K.; Nakasuji, K.; Naito, A. *Synth. Met.* **1999**, *103*, 2257.

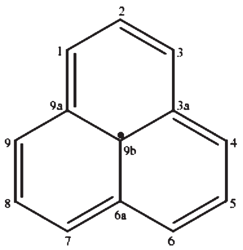

**Figure 1.** Localized representation of the phenalenyl radical, *P*.

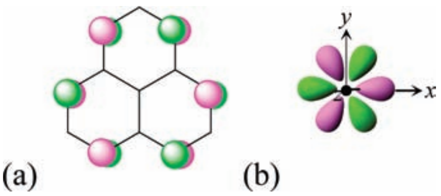

**Figure 2.** (a) Representation of the SOMO of the phenalenyl radical (b) Representation of the $f_{x(x^2-3y^2)}$ orbital of $\phi$ axial symmetry.

slightly shorter (~0.1 Å) than the typical aromatic C——C van der Waals distance.[11−13] Experimental evidence is available for a stable $\sigma$ dimer, as well, in which one of the secondary carbon atoms involved in the SOMO of one phenalenyl radical (see Figure 2) bonds to an identical site on another phenalenyl radical.[13b,14]

**High Symmetry Bonding Possibilities.** Looking at the SOMO depicted in Figure 2a, one might envision the formation of symmetric *P*—M half sandwich, or *P*—M—*P* sandwich structures (analogues of the metallocenes) in which M has orbitals of the right symmetry to overlap equally with the six lobes of the SOMO of *P*. However, s, p, and d orbitals on transition metals do not have the right ($D_{3h}$) symmetry to match the six equivalent lobes of the SOMO of *P*. One has to go further down the periodic table, to the actinides, to find metal atoms with f valence orbitals, some of which are indeed of the requisite symmetry. Figure 2b shows one of the relevant f orbitals of $\phi$ axial symmetry.

There is an analogy here to the fascinating electronic structure of the uranocenes pioneered by Streitweiser and Mueller−Westerhoff.[15,16] In those systems, the uranium f $\delta$ orbitals and other f and d orbitals play a key role in the bonding.[15]

Nonetheless, the f orbitals of the actinide atoms are characteristically difficult bonding partners. They are contracted in toward the nucleus such that the d orbitals that are close by in energy are often better contenders for bonding, if symmetry conditions allow.[17]

We examine briefly the influence of the (limited) radial extent of the actinide f $\phi$ orbital on the bonding of the metal with *P* to form symmetric sandwich-type structures that involve the SOMO on *P* and the actinide f orbitals, using uranium as our metal of choice.

Our primary objective, however, is to explore the structure, bonding, and energetics of a class of bis(phenalenyl) ($MP_2$) complexes of divalent metals in which the phenalenyl radicals are formally one electron acceptors. The metals we consider are those of groups 2 and 12. We examine, as well, the modifications in the bonding as we go from M = Ca to M = Zn across the first row transition metal series. We have been surprised to find in the literature no experimental or theoretical treatment of the metal-bis(phenalenyl) $MP_2$ systems; a remotely related study examines a Cu complex in which two linked aza-derivatives of the phenalenyl radical are coordinated to the metal via two N sites.[14]

**Lower Symmetry Bonding Possibilities (with Groups 2 and 12 Metals).** The groups two and twelve metals are known to form $MR_2$ sandwich type and simple binary triatomic molecules with a significant degree of structural diversity. The group 2 dihalides ($MX_2$: M = Be, Mg, Ca, Sr, and Ba; X = F, Cl, Br, and I), for instance, are linear for M = Be and Mg, but are bent for several of the heavier metals: $CaF_2$, $SrF_2$, $SrCl_2$, and the $BaX_2$ molecules are all bent.[18] This observation has been rationalized successfully by an increased involvement of $(n-1)$d-orbitals in the bonding as M gets larger,[19−21] and by the influence of core-polarization interactions between the M and X sites.[20,22] An explanation rooted in the pseudo-Jahn−Teller effect has been proposed recently.[23]

The bis(cyclopentadienyl) complexes (the metallocenes) of the group 2 metals show, as well, a significant sensitivity to the position of the metal in the periodic table.[24−27] Beryllocene, first prepared 50 years ago in E. O. Fischer's lab,[28] is a slip sandwich complex[24,25] in which the beryllium has a pentahapto ($\eta^5$) bond to one of the cyclopentadienyl (Cp) rings and a simple ($\eta^1$) covalent bond to a single carbon on the other Cp ring (structure 1 in Figure 3).[29−31]

---

(13) (a) Suzuki, S.; Morita, Y.; Fukui, K.; Sato, K.; Shiomi, D.; Takui T.; Nakasuji, K.; *J. Am. Chem. Soc.* **2006**, *128*, 2530, and references therein. (b) Small, D.; Rosokha, S. V.; Kochi, J. K.; Head-Gordon, M. *J. Phys. Chem. A*. **2005**, *109*, 11261.

(14) Zheng, S.; Lan, J.; Khan, S. I.; Rubin, Y. *J. Am. Chem. Soc.* **2003**, *125*, 5786.

(15) Streitwieser, A.; Mueller-Westerhoff, U. *J. Am. Chem. Soc.* **1968**, *90*, 7364.

(16) Zalkin, A.; Raymond, K. N. *J. Am. Chem. Soc.* **1969**, *91*, 5667.

(17) Gagliardi, L.; Pyykkö, P. *Angew. Chem., Int. Ed.* **2004**, *43*, 1573.

(18) (a) Wharton, L; Berg, R. A.; Klemperer, W. *J. Chem. Phys.* **1963**, *39*, 2023. (b) Büchler, A.; Stauffer, J. L.; Klemperer, W. *J. Chem. Phys.* **1964**, *40*, 3471. (c) Büchler, A.; Stauffer, J. L.; Klemperer, W. *J. Am. Chem. Soc.* **1964**, *86*, 4544.

(19) DeKock, R. L.; Peterson, M. A.; Timmer, L. K.; Baerends, E. J.; Vernooijs, P. *Polyhedron* **1990**, *9*, 1919 (and references therein); **1991**, *10*, 1965 (erratum).

(20) (a) Kaupp, M. *Angew. Chem., Int. Ed.* **2001**, *40*, 3535. (b) Hargittai, M. *Chem. Rev.* **2000**, *100*, 2233.

(21) (a) von Szentpály, L.; Schwerdtfeger, P. *Chem. Phys. Lett.* **1990**, *170*, 555. (b) Kaupp, M.; Schleyer, P. v. R.; Stoll, H.; Preuss, H. *J. Am. Chem. Soc.* **1991**, *113*, 6012.

(22) (a) Guido, M.; Gigli, G. *J. Chem. Phys.* **1976**, *65*, 1397. (b) Donald, K. J.; Mulder, W. H.; von Szentpály, L. *J. Chem. Phys.* **2003**, *119*, 5423. (c) In ref 21a, von Szentpály, and Schwerdtfeger suggested that explanations from d orbital involvement and core polarization were "two sides of the same coin". Kaupp echoes this perspective on p 3544 of ref 20a.

(23) Garcia-Fernandez, P.; Bersuker, I. B.; Boggs, J. E. *J. Phys. Chem. A* **2007**, *111*, 10409.

(24) Beattie, J. K.; Nugent, K. W. *Inorg. Chim. Acta* **1992**, *198*, 309.

(25) Jutzi, P.; Burford, N. *Chem. Rev.* **1999**, *99*, 969.

(26) Sapunov, V. N.; Kirchner, K.; Schmid, R. *Coord. Chem. Rev.* **2001**, *214*, 143.

(27) Rayón, V. M.; Frenking, G. *Chem.—Eur. J.* **2002**, *8*, 4693.

(28) Fischer, E. O.; Hofmann, H. P. *Chem. Ber.* **1959**, *92*, 482.

(29) (a) Almenningen, A.; Haaland, A.; Lusztyk, J. *J. Organomet. Chem.* **1979**, *170*, 271. (b) Gleiter, R.; Böhm, M. C.; Haaland, A.; Johansen, R.; Lusztyk, J. *J. Organomet. Chem.* **1979**, *170*, 285. (c) Lusztyk, J.; Starowieyski, K. B. *J. Organomet. Chem.* **1979**, *170*, 293. (d) Nugent, K. W.; Beattie, J. K.; Hambley, T. W.; Snow, M. R. *Aust. J. Chem.* **1984**, *37*, 1601. (e) Sanz, J. F.; Márquez, A. M. *Theor. Chem. Acc.* **2006**, *116*, 480.

(30) Hanusa, T. P. *Organometallics* **2002**, *21*, 2559.

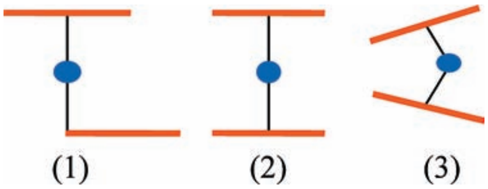

**Figure 3.** (Experimental or Computed) Structural preferences in the group 2 metallocene: (1) $BeCp_2$, (2) $MgCp_2$ ($CaCp_2$, and $SrCp_2$, have a very low barrier to bending), and (3) $BaCp_2$.

Magnesocene ($MgCp_2$)[32] is a linear sandwich complex structurally identical to ferrocene.[25,32] The unavailability of accurate experimental geometrical data for the heavier group 2 metallocenes (all reported by Fischer and Stölzle in 1961[33]) is explained in part by the low volatility of the compounds.[34] Nevertheless, theoretical calculations at the HF and MP2 levels find floppy but linear sandwich structures for $CaCp_2$ and $SrCp_2$, and a bent minimum energy sandwich structure for $BaCp_2$ with a very low barrier to linearization (1.39 kJ/mol).[25,35]

Like the Be and Mg dihalides, the group 12 dihalides are all linear[36] (see ref 20 and references therein). As far as we know, gas phase experimental data is unavailable for unsubstituted $CdCp_2$ and $HgCp_2$; however, mounting evidence, including recent electron diffraction data, indicate that $ZnCp_2$ prefers, like $BeCp_2$, the slip-sandwich ($\eta^1$,$\eta^5$) structure.[37,38]

The minimum energy structures of the bis(phenalenyl) groups 2, 12 and transition metal complexes show a remarkable diversity in their structural preferences. We find a stunning variety of bonding motifs, including $\eta^1$,$\eta^2$ and $\eta^3$ type M—$P$ interactions and bent sandwich complexes. The bonding and energetics in this class of complexes shows an acute dependence on the spatial extent of the atomic orbitals of the metal, and the availability of empty $(n-1)$d and $n$p orbitals. The Be, Ca, Sr, Ba, and the transition metal $MP_2$ complexes are expected to be stable thermodynamically at ambient conditions (Supporting Information, Table S.1).

## Method

The computational results reported in this work, including all geometrical parameters, binding enthalpies, and natural bond orbital (NBO)[39] analysis data, have been obtained using the Becke three parameter hybrid functional, with correlation provided by Lee, Yang, and Parr (The B3LYP method)[40] and an ultrafine grid. The 6-31G* basis set was employed for the smaller atoms, H, Be, and C,[41] and the 6-311G* basis set for Mg.[42] For competitive isomers of Be$P_2$ and Mg$P_2$, that is, for local minima on the potential surfaces that are very close in energy, the structural preferences were confirmed by repeating the geometry optimizations and vibrational analyses using larger basis sets. The basis sets use were (i) the 6-311G* and (ii) the correlation consistent triple-ζ (cc-pVTZ) basis sets[43] for all the atoms in the complexes.

For Ca, Sr, Ba, and the d-block elements, we used scalar-relativistic energy-consistent small core Dirac−Fock (MDF) effective-core pseudopotentials (ECPs): 10*e*-, and 28*e*- cores for elements in the period 4 and 5, respectively; a 46*e*- core for Ba, and a 60*e*- core for Hg (without the spin−orbit potential but including the scalar relativistic effects), and the corresponding basis sets.[44] Computed binding energies and enthalpies reported in this work have been adjusted for basis set superposition errors (BSSEs) by the addition of counterpoise corrections ($\delta^{CP}$)[45] to the computed values. All the calculations were performed using the Gaussian 03 suite of programs.[46] The orbital pictures have been generated using the GaussView graphics software.[47]

## Results and Discussion

The SOMO of the phenalenyl radical clearly has the requisite $D_{3h}$ symmetry (Figure 2a) for bonding with actinide 5f $\phi$ ($f_{x(x^2-3y^2)}$ or $f_{y(y^2-3x^2)}$) valence orbitals (Figure 2b). However, the size of $P$ makes it difficult for a single atom to bond symmetrically with the SOMO, which is restricted to alternating carbon sites on the large twelve carbon ring (Figure 2a).

**Close, But Not Close Enough.** The carbon $2p_z$ orbitals involved in the SOMO of $P$ (see Figure 2a) are each about 2.5 Å away from the central C atom (that is, $a \approx 2.5$ Å in Figure 4).[48] So, for a given metal atom, M, located some

---

(31) In ref 24, Beattie and Nugent, suggest that the diversity in the structural preferences in main group metallocenes is explained by a competition between certain factors: (See ref S.1).

(32) (a) Weiss, E.; Fischer, E. O. *Z. Anorg. Allg. Chem.* **1955**, *278*, 219. (b) Pinkus, A. G. *J. Chem. Educ.* **1978**, *55*, 704: A brief discussion of the structure and ionic character of magnesocene, this reference provides a bibliography of works on metallocenes before 1978.(c) Jaenschke, A.; Paap, J.; Behrens, U. *Z. Anorg. Allg. Chem.* **2008**, *634*, 461.

(33) Fischer, E. O.; Stolzle, G. *Chem. Ber.* **1961**, *94*, 2187.

(34) Blom, R.; Faegri, K.Jr.; Volden, H. V. *Organometallics* **1990**, *9*, 372.

(35) (a) Kaupp, M; Schleyer, P. v. R.; Dolg, M.; Stoll, H. *J. Am. Chem. Soc.* **1992**, *114*, 8202. (b) Experimental data for the bis(pentamethylcyclopentadienyl) (Cp*) complexes of Ca, Sr, and Ba suggest bent sandwich structures in each case with Cp*(ring center)—M—Cp*(ring center) angles between 154° (for $CaCp^*_2$) and 148° (for $BaCp^*_2$) (see refs 22a, 25, and 34).

(36) Donald, K. J.; Hargittai, M.; Hoffmann, R. *Chem.—Eur. J.* **2009**, *15*, 158.

(37) (a) Blom, R.; Haaland, A.; Weidlein, J. *J. Chem. Soc., Chem. Commun.* **1985**, 266. (b) See p 983 in ref 25. A similar ($\eta^5\eta^1$) structure has been obtained for the ZnCp* complex.

(38) Haaland, A.; Samdal, S.; Tverdova, N. V.; Girichev, G. V.; Giricheva, N. I.; Shlykov, S. A.; Garkusha, O. G.; Lokshin, B. V. *J. Organomet. Chem.* **2003**, *684*, 351.

(39) (a) Carpenter, J. E.; Weinhold, F *J. Mol. Struct.: THEOCHEM* **1988**, *169*, 41. (b) Reed, A. E.; Curtiss, L. A.; Weinhold, F. *Chem. Rev.* **1988**, *88*, 899, and references therein.

(40) (a) Becke, A. D. *J. Chem. Phys.* **1993**, *98*, 5648. (b) Lee, C.; Yang, W.; Parr, R. G *Phys. Rev. B* **1988**, *37*, 785.

(41) For a description of the structure of the 6-31G* basis sets see: Hariharan, P. C.; Pople, J. A. *Theor. Chim. Acta* **1973**, *28*, 213.

(42) (a) Krishnan, R.; Binkley, J. S.; Seeger, R.; Pople, J. A. *J. Chem. Phys.* **1980**, *72*, 650. (b) McLean, A. D.; Chandler, G. S. *J. Chem. Phys.* **1980**, *72*, 5639.

(43) (a) Dunning, T. H.Jr. *J. Chem. Phys.* **1989**, *90*, 1007. (b) Woon, D. E.; Dunning, T. H.Jr. *J. Chem. Phys.* **1993**, *98*, 1358.

(44) (a) Dolg, M.; Wedig, U.; Stoll, H.; Preuss, H. *J. Chem. Phys.* **1987**, *86*, 866. (b) Figgen, D.; Rauhut, G.; Dolg, M.; Stoll, H. *Chem. Phys.* **2005**, *311*, 227. (c) Lim, I. S.; Stoll, H; Schwerdtfeger, P. *J. Chem. Phys.* **2006**, *124*, 034107. These basis sets are all available electronically at the website of the institute for theoretical chemistry in Stuttgart: http://www.theochem.uni-stuttgart.de/pseudopotentials/clickpse.en.html.

(45) The computed counterpoise corrections $\delta^{CP}$ were obtained directly from our density functional calculations using the Gaussian 03 program. The definition of $\delta^{CP}$ and steps involved in calculating it are outlined in: Jensen, F. *Introduction to Computational Chemistry*; Wiley: New York, 1999; pp 172−173. The corrected binding enthalpies, $\Delta H_{bind}$, $= H^{CP}(MP_2) - [H(M) + 2H(P)]$, where $H^{CP}(MP_2) = H(MP_2) + \delta^{CP}$.

(46) Frisch, M. J. et al. *Gaussian 03*, Revision E.01; Gaussian, Inc.: Pittsburgh, PA, 2003; (complete citation in Supporting Information, ref. S.2).

(47) The GaussView (3.0 and 4.1) graphics program has been used to plot the molecular orbital diagrams in this report. In each case, unless otherwise indicated, the settings used are (isosurface) isovalue = 0.02 and cube grid = medium.

(48) If the C—C bond distance is taken to be 1.45 Å, the distance between atoms 9b and 9 for instance (as numbered in Figure 1) is 2 × cos(30) × 1.45 Å = 2.5 Å.

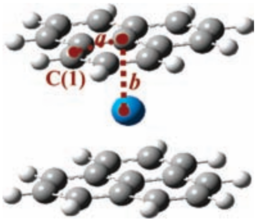

**Figure 4.** Hypothetical U$P_2$ structure with $D_{3d}$ symmetry.

distance $b$ along the principal $C_3$ axis of the *hypothetical* complex shown in Figure 4, the M—C(1) contact is $c = (a^2 + b^2)^{1/2}$.

We find, however, that even if we accept a rather short distance between the metal atom and the central carbon atom, ($b$ = 2.6 Å),[49] the separation, $c$, between the uranium atom and C(1) or any of the other equivalent carbon sites around the ring would be too long for a U−C bonding contact: $c \approx (2.5^2 + 2.6^2)^{1/2}$ Å = 3.6 Å. This distance is ~0.85 Å longer than the U−C bond in Uranocene[16] and in the recently characterized $[(C_5Me_5)_2U(NCMe)_5]^{2+}$ linear sandwich complex.[50] So, the SOMO (Figure 2a) and other molecular orbitals (MOs) located on the periphery of $P$ are too spread out to bond successfully with the U atom or to other actinides with comparable or smaller atomic radii.

**Spatial Incompatibility Illustrated.** The incompatibility of the U metal f $\phi$ orbital and the SOMO of $P$ may be illustrated further using a hypothetical U$P_2$ structure of $D_{3d}$ symmetry (like that shown in Figure 4). From symmetry considerations, one expects that the linear U$P_2$ sandwich structure will have an $\mathrm{A}'_{1u}$ orbital built entirely from one metal f $\phi$ orbital and the SOMO of both of the $P$ fragments. One iso-surface of this molecular orbital is shown in Figure 5 (with $b$, the distance between the central carbon (site (9b) in Figure 1) and the U atom arbitrarily set at 2.64 Å).

The top view of the molecular orbital (Figure 5b) shows an obvious area of low electron density in the middle of the $P$ fragments. The metal f $\phi$ orbital, sandwiched by these areas of low charge density, is in a void, a "hollow" region in which the SOMO on the periphery is effectively out of reach. The radial function of the metal f orbital falls off rather rapidly, and extends outward to overlap only very weakly with the carbon $p_z$ orbitals. Thus, the $D_{3d}$ symmetric sandwich structure (Figures 4 and 5), its beauty notwithstanding, is hardly a tenable molecular geometry for an actinide$P_2$ complex.[51] Even so, as we will see in the following sections, the phenalenyl radical has several remarkable lower symmetry bonding options.

**Bis(phenalenyl) Complexes Involving Divalent Metals.** The stability of the phenalenyl radical (and its anion) suggest the possibility of forming a neutral M$P_2$ complex in which the $P$ radicals are electron acceptors ($P^-$) bonded in some (likely non-symmetrical) fashion to a divalent metal.[52] We carried out a series of structural studies on the metal bis(phenalenyl), M$P_2$, complexes of the groups 2 and 12 metals and observed significant variations in the structural preferences in the complexes going down group 2 from Be to Ba and across the periodic table to the group 12 metals.

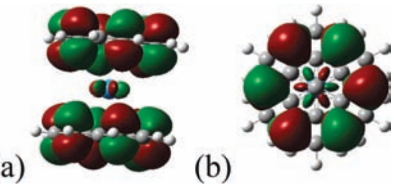

**Figure 5.** $\mathrm{A}'_{1u}$ MO of a *hypothetical* (single point) U$P_2$ complex with $D_{3d}$ symmetry: (a) side view and (b) top view.

**Structural Diversity in Bis(phenalenyl) Group 2 Metal Complexes. Be$P_2$ Complexes.** The two most stable isomers we identified on the Be$P_2$ potential energy surface are $\eta^1,\eta^3$ type complexes. Another (slightly higher energy) local minimum is a slip sandwich $\eta^1,\eta^1$ type structure. A discussion of these systems will lay the foundation for our assessment of the bonding in the other group 2 and the group 12 metal complexes we will meet in later sections.

**$\eta^1,\eta^3$.** The two lowest energy Be$P_2$ structures[53] are unexpected $\eta^1,\eta^3$ systems with $C_1$ symmetry (see the Supporting Information, Figure S.1a). The two complexes ($C_1$(1) (Figure 6) and $C_1$(2) (Supporting Information, Figure S.1b)) are rotamers of each other, with the latter being higher in energy by only 0.01 eV. Since the $\eta^1,\eta^3$ bonding motif is common to both structures, we describe only the more stable ($C_1$(1)) structure in detail (Figure 6; cf. Supporting Information, Figure S.1b).

In Figure 6, the Be atom bonds in very different ways to the two phenalenyl rings. The highest occupied molecular orbital (HOMO) in Figure 6 involves the Be atom and $P'$ only (lower left, Figure 6); a simple $\sigma$ overlap between a beryllium sp hybrid orbital and the $p_z$ orbital of a single carbon atom in the $\pi$ system of $P'$.[54] The HOMO-1 is remarkably different. It involves a $\sigma$ *side-on bridging interaction* between a beryllium p orbital that is parallel to the plane of $P''$ and two carbon 2p orbitals that are meta- to each other and involved in the SOMO of $P''$ (Figure 6).

We describe the Be—$P''$ bond formally as $\eta^3$, but must emphasize that the decisive interaction is between the beryllium atom and carbons (1) and (3) only (Figure 7).

The unusual $\eta^3$ Be—$P''$ interaction has a strong connection to the $\eta^3$-type metal-allyl bonding motif, of which the literature is replete with examples (starting from the 1959 report by Smidt and Hafner[55]).[56] The $C_3H_5$ allyl ligand, viewed as an anion ($C_3H_5^-$), has a filled $\pi$-type HOMO that has a node on the central atom analogous to the three carbon fragment on $P''$ shown in Figure 7. Indeed, the $P'$Be$P''$ molecule may be described, locally, as an ($\eta^1,\eta^3$) R—Be—allyl complex, if we ignore weaker interactions of the Be atom with the rest of the phenalenyl rings.

---

(49) The U—C van der Waals contact is ~ (1.90 Å (U) + 1.70 Å (C)) = 3.60 Å.

(50) Maynadié, J.; Berthet, J.-C.; Thuéry, P.; Ephritikhine, M. *J. Am. Chem. Soc.* **2006**, *128*, 1082.

(51) Geometry optimizations performed on a few phenalenyl complexes with U in more realistic oxidation states generated rather interesting minimum structures (See Supporting Information, ref S.3).

(52) The stability of the phenalenyl cation, $P^+$, implies that $P^+{}_2R^{2-}$ complexes in which $P$ is an electron donor may be stable, as well.

(53) For details on how we converged on the $\eta^1,\eta^3$ structure see Supporting Information, ref S.4.

(54) For comments on the structural effects of the ~$sp^2 \rightarrow sp^3$ hybridization in M$P_2$ see Supporting Information, ref S.5.

(55) Smidt, J.; Hafner, W. *Angew. Chem.* **1959**, *71*, 284.

(56) Elschenbroich, C. *Organometallics*, 3rd ed.; Wiley-VCH: Weinheim, Germany, 2006; allyl complexes pp 436 ff; Main group metallocenes pp 59 ff.

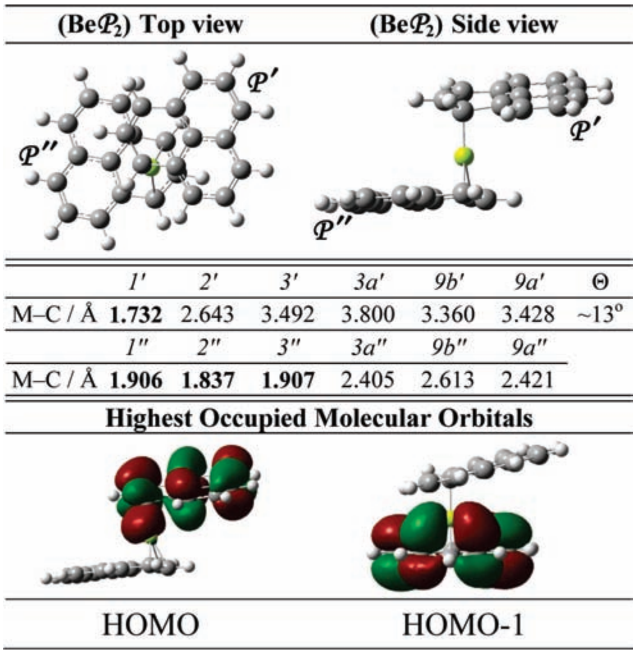

| | 1′ | 2′ | 3′ | 3a′ | 9b′ | 9a′ | Θ |
|---|---|---|---|---|---|---|---|
| M–C / Å | **1.732** | 2.643 | 3.492 | 3.800 | 3.360 | 3.428 | ~13° |
| | 1″ | 2″ | 3″ | 3a″ | 9b″ | 9a″ | |
| M–C / Å | **1.906** | **1.837** | **1.907** | 2.405 | 2.613 | 2.421 | |

**Figure 6.** Lowest energy ($\eta^1$,$\eta^3$) Be$P_2$ isomer (C$_1$(1)) and key frontier molecular orbitals. The numerical labels refer to the phenalenyl carbon sites following the assignments in Figure 1. The indices ′ and ″ distinguish between the two $P$ groups. Θ is an estimate of the angle between the planar 10 carbon naphthalene fragments outside the bonding region of the complex.

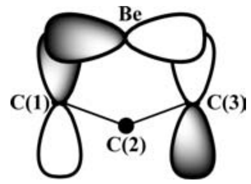

**Figure 7.** Simple representation of the key Be—$P''$ interaction.

**$\eta^1$,$\eta^1$.** The $C_i$ $\eta^1$,$\eta^1$ isomer shown in Figure 8 is higher in energy than $C_1$(1) by just ~0.08 eV (~1.8 kcal mol$^{-1}$). It is built up from two $\sigma$ bonds involving an sp hybridized beryllium atom and a single carbon atom on each of the two phenalenyl radicals. The two highest occupied MOs of this complex (see Supporting Information, Figure S.2) confirm that the Be 2s and 2p orbitals participate in the Be−C bonds.

**(In)stability of the $\eta^1$,$\eta^1$ Isomer.** Figure 9 shows the outcome of a linear transit from the preferred $\eta^1$,$\eta^3$ structure to the $\eta^1$,$\eta^1$ complex. Notice that the cost in energy to go from one $\eta^1$,$\eta^3$ structure to the next $\eta^1$,$\eta^3$ structure ($C_1$(1) ↔ $C_1$(2)) is very low (~ 0.02 eV).

This motion is expected to be essentially barrierless, at moderate temperatures. Indeed, frequency analyses of the two $\eta^1$,$\eta^3$ complexes ($C_1$(1) and $C_1$(2)) reveal that the lowest frequency normal mode in each case is a twisting motion of the phenalenyl rings relative to each other, exactly the motion involved in going from one of these rotamers to the next (Supporting Information, Figure S.1a).

The energy separation between the $\eta^1$,$\eta^3$ structures and the $\eta^1$,$\eta^1$ system is only ~0.08 eV, but the barrier between them is much higher (~0.43 eV (9.8 kcal mol$^{-1}$); Figure 9). This barrier (going from the $\eta^1$,$\eta^3$ to the $\eta^1$,$\eta^1$ structures) is explained by the high cost in energy to (i) break the multicenter Be—$P''$ bond (Figure 6) and (ii) rehybridize (from ~sp$^2$ toward sp$^3$) at a carbon atom in $P''$ in preparation to form the second $\eta^1$ $\sigma$ Be−C bond (to give a $\eta^1$,$\eta^1$ structure (Figure 8)). We calculate a preparation energy of 0.79 eV (18.2 kcal mol$^{-1}$) for one of the distorted phenalenyl fragments in the $\eta^1$,$\eta^1$ structure, relative to the isolated ground state radical.

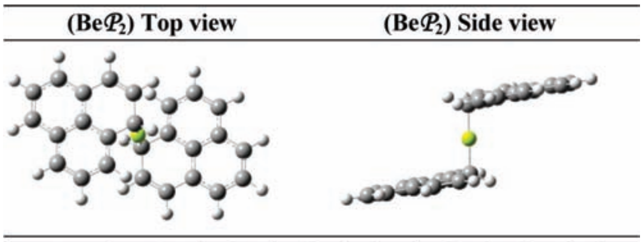

| | 1 | 2 | 3 | 3a | 9b | 9a | Θ |
|---|---|---|---|---|---|---|---|
| M–C / Å | **1.704** | 2.499 | 3.320 | 3.683 | 3.335 | 2.471 | 0.0° |

**Figure 8.** Minimum energy ($C_i$) structure of the bis(phenalenyl)beryllium complex (the C atoms are labeled following the assignments in Figure 1).

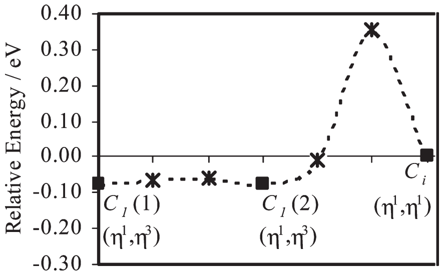

**Figure 9.** Linear transit, from the (C$_1$(1)) $\eta^1$,$\eta^3$ to the (C$_i$) $\eta^1$,$\eta^1$ complex, obtained using the Synchronous Transit-Guided Quasi-Newton (STQN) Method (using the QST3; Path = 7 conditions) as implemented in Gaussian 03.

Of course, the actual formation of the new Be−C ($\eta^1$) $\sigma$ bond is stabilizing. However, the preference for the $\eta^1$,$\eta^3$ structure indicates that this stabilization fails to overcompensate for the cost of breaking the $\eta^3$ bond and the necessary rehybridization. The preference for the $\eta^1$,$\eta^3$ structure over the $\eta^1$,$\eta^1$ option is, therefore, the outcome of a compromise, a trade off between the strength of the Be—$P$ interactions in the molecule and the cost of preparing the phenalenyl fragment for bonding to Be. This compromise explains, as well, the preference in the BeCp$_2$ complex for an $\eta^1$,$\eta^5$ instead of an $\eta^1$,$\eta^1$ geometry.[24,25]

**Mg$P_2$: a Metal Mediated Dimer?** The bis(phenalenyl) magnesium complex presents a different picture. The Mg$P_2$ analogue of the $\eta^1$,$\eta^3$ Be$P_2$ structure (Figure 6) is only a local minimum on the Mg$P_2$ potential energy surface. Structural optimizations performed at the B3LYP level of theory using different (6-311G* or cc-pVTZ) basis sets for all (Mg, C, and H) atoms in the complex confirm that the $\eta^1$,$\eta^3$ structure is higher in energy (by some 0.10 to 0.15 eV) relative to an $\eta^6$,$\eta^6$ alternative (Figure 10). A second $\eta^6$,$\eta^6$ minimum energy structure that we obtained (Supporting Information, Figure S.3) has a slightly larger overlap between the phenalenyls and is 0.02 eV higher in energy.[57]

---

(57) A transition state structure, an eclipsed rotamer midway between the staggered $\eta^6$,$\eta^6$ structure in Figure 11 and its stereoisomer, is shown in Supporting Information, Figure S.4a,b.

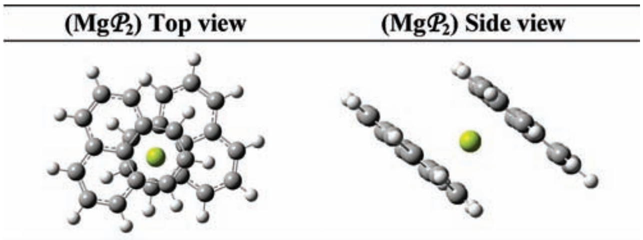

| | *1* | *2* | *3* | *3a* | *9b* | *9a* | Θ |
|---|---|---|---|---|---|---|---|
| M–C / Å | 2.361 | 2.325 | 2.343 | 2.542 | 2.609 | 2.550 | 0.0° |

**Figure 10.** Preferred structure of the Mg$P_2$ complex (the C atoms are labeled following the assignments in Figure 1). Key molecular orbitals are shown in Supporting Information, Figure S.5.

In the minimum energy $\eta^6,\eta^6$ structure (Figure 10), the Mg atom is nestled in a local $\sim D_{6d}$ environment, between the two staggered six-membered rings, which are ~4.0 Å apart.[58] We find, however, that the bonding between the metal and the phenalenyl rings is rather weak.

A compelling piece of geometrical evidence of a weak interaction between the metal and the rings is the fact that, in the Mg—$P$ bonding region, the phenalenyl ring is hardly perturbed structurally. As we will show in later sections, computed binding enthalpies and an NBO analysis[39] confirm that the covalent contribution to the Mg—$P$ interaction is relatively small, and that the Mg$P_2$ complex is slightly unstable thermodynamically. Indeed, the frontier molecular orbitals of the complex (Supporting Information, Figure S.5) show no significant Mg—$P$ bonding interaction; considering the long sausage-like $P$—$P$ overlap regions (Supporting Information, Figure S.5) that almost completely exclude the Mg atom, the complex may be described simply as a weakly bound Mg mediated $P_2$ dimer.

**M$P_2$ Bent Sandwich Complexes of Ca, Sr, and Ba.** The minimum energy structures obtained from several starting geometries for M = Ca, Sr, and Ba are bent sandwich complexes stabilized by bonding interactions between the metal (predominantly d) orbitals and the $p_z$ orbitals of the phenalenyl SOMO.

The structure of the Ca complex and the geometrical parameters for the analogous Sr and Ba bent bis(phenalenyl) complexes are shown in Figure 11. The two highest occupied molecular orbitals of the Ca, Sr, and Ba complexes (Supporting Information, Figure S.6) illustrate clearly the central role of the ($n$ − 1)d orbitals in the bonding in the bis(phenalenyl) complexes of these heavier group 2 metals.

The main distinction between the Be and Mg systems and these Ca, Sr, and Ba complexes is the strong preference in the latter for the (high hapticity) bent structure. As we mentioned in the introduction, a similar situation is observed in the group 2 metallocenes and several of their derivatives. In these bent bis(phenalenyl) complexes, the bending increases rapidly going down group 2 from M = Ca to M = Ba. The computed interplanar angle between the two $P$ groups[59] (= 0.0° for parallel rings) is 9°, 12°, and 21° for the Ca, Sr, and Ba complexes, respectively.

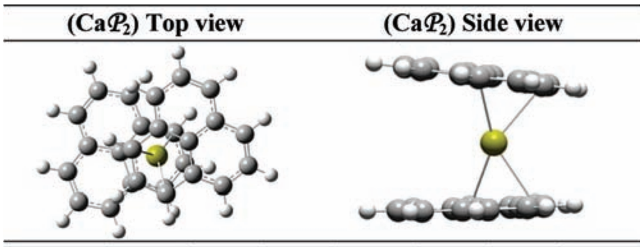

| | *1* | *2* | *3* | *3a* | *9b* | *9a* | *Θ* |
|---|---|---|---|---|---|---|---|
| Ca–C / Å | *2.653* | *2.677* | *2.654* | *2.744* | *2.769* | *2.739* | *~9°* |
| Sr–C / Å | 2.838 | 2.868 | 2.829 | 2.877 | 2.889 | 2.879 | 12° |
| Ba–C / Å | 3.056 | 3.075 | 3.004 | 3.014 | 3.040 | 3.068 | 21° |

**Figure 11.** Minimum energy structure and key frontier molecular orbitals of the bis(phenalenyl)calcium complex and the structural data for the bent Sr and Ba bis(phenalenyl) analogues (the C atoms are identified according to the labeling system used in Figure 1).

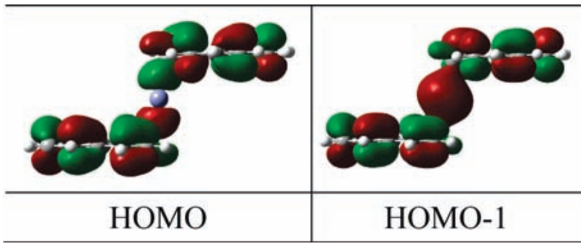

**Figure 12.** Frontier molecular orbitals of the minimum energy structure of the zinc bis(phenalenyl) complexes. Identical frontier MOs are obtained for all the group 12 complexes.

Going from Ca to Ba there is a significant decrease in the energy separation between the occupied metal s orbitals and the empty d orbitals. This orbital effect is crucial for explaining the structural preferences in these systems; the availability of metal ($n$ − 1)d orbitals for bonding is as decisive for the bending in the group 2 metal bis(phenalenyl) complexes as it is for the bending in the group 2 dihalides and metallocenes.[19−21,35,36]

The increased bending in the complexes going from Ca to Ba is explained by (i) an increased participation of the d orbitals in bonding and (ii) an improved overlap between key carbon sites in the $P'$ groups and the metal $n$s($n$ − 1)d hybrid orbitals as M gets larger, plus (iii) a decrease in the $P$—$P$ repulsion as the M—$P$ contacts get longer.

**Group 12 Bis(phenalenyl) Slip-Sandwich Complexes.** A search for the possible minimum energy structures of group 12 M$P_2$ complexes from various starting geometries led us repeatedly to an $\eta^1,\eta^1$ type slip sandwich complex (Figure 12; Supporting Information, Figure S.7a,b) analogous to the $C_i$ ($\eta^1,\eta^1$) Be$P_2$ structure in Figure 8. In these group 12 complexes, the metal is bonded to only a single C site on each of the phenalenyl rings with M—C bond distances of 2.012 Å, 2.243 Å, and 2.260 Å for M = Zn, Cd, and Hg, respectively.

The preference in the group 12 bis(phenalenyl) complexes for this $\eta^1,\eta^1$ structure is straightforward to interpret. The metal d orbitals, which are completely filled in the group 12 metals, are hardly involved in the bonding in these complexes. The bonding molecular orbitals in the group 12 complexes (Figure 12) are built up from a $\sigma$ overlap between the $2p_z$ orbital of a carbon on each of the phenalenyl rings and the metal $n$s and $np_z$ orbitals. It is clear from the HOMO (on the left in Figure 12), however,

---

[58] This $P$—$P$ separation is comparable to Cp—Cp separations of ~4.0 Å in bis(cyclopentadienyl) magnesium and its derivatives.

[59] See Supporting Information, ref S.6 for a summary of how the interplanar angles were obtained.

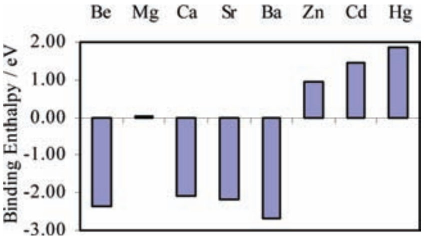

**Figure 13.** BSSE corrected binding enthalpies for the lowest energy groups 2 and 12 M$P_2$ complexes.[45]

that the metal $p_z$ orbital plays a rather small role in the bonding. In fact, the HOMO is almost entirely on the $P$ fragments in the Zn complex (Figure 12). The picture is quite the same for M = Cd and Hg (see Supporting Information, Figure S.8). We see in the next sections that the poor involvement of the metal $n$p orbitals in the bonding has significant consequences for the stability of the group 12 complexes.

**Stability of the Groups 2 and 12 M$P_2$ Complexes.** The inferences we have made so far about the stability of the bis(phenalenyl) complexes have been based largely on structural evidence and the nature of the frontier MOs. To improve our understanding of the bonding in these complexes, we computed the BSSE corrected binding energies and enthalpies for the lowest energy M$P_2$ isomers for each M (Supporting Information, Table S.1; Figure 13).

The thermochemical data in Figure 13 supports strongly our preliminary assessment of the bonding situation in the complexes. The binding enthalpies obtained for all three of the elegant $\eta^1$,$\eta^1$ group 12 bis(phenalenyl) complexes are large and positive: the complexes are therefore quite unstable (by 0.94 to 1.86 eV; see Figure 13 and Supporting Information, Table S.1), relative to the isolated M and $P$ radicals.

Among the group 2 bis(phenalenyl) complexes, the minimum energy magnesium complex is exceptional. The binding enthalpy is small and positive ($\Delta H$ = +0.02 eV) so that Mg$P_2$ is expected to be thermodynamically unstable at ambient conditions. The ($\eta^1$,$\eta^3$) Be complex and the bent Ca, Sr, and Ba systems are predicted to be quite stable, however, with $\Delta H < -2.0$ eV for all four of those systems.

A detailed study of the potential energy surfaces of these bis(phenalenyl) complexes is expensive, and is complicated by a difficulty in identifying and optimizing first-order saddle points that directly link the complex and the isolated metal and $P$ radicals. The upper limits of the barriers to dissociation have been estimated, nonetheless, by computing the energy separation $E_{\text{barrier}} = (2E(P^*) + E(\text{M}^*)) - E(\text{M}P_2)$ between the M$P_2$ complex and the promoted reference fragments. Here M* is the triplet ($n$s$n$p or $n$s($n$ − 1)d) metal, and $P$* is the distorted P fragment as it is in the complex. We obtain a dissociation barrier of 3.01 eV for M = Mg compared to 6.07 eV (M = Be) to 3.88 eV (M = Ba) for the other group 2 compounds (see Supporting Information, Table S.2).

Our assumption of a 50% $n$p or ($n$ − 1)d involvement (sp or sd) in the metal hybrid orbitals is crucial for the barriers we obtain, however, especially for M = Mg. If, for instance (at an extreme), we use the unhybridized (singlet) metal as our reference, the barrier falls from 3.01 eV to just 0.23 eV for M = Mg. The barrier shrinks for all the group 2 metal complexes when we use the unhybridized reference, but remains relatively high (between 3.6 to 2.4 eV; Supporting Information, Table S.2) for M = Be, Ca, Sr, and Ba. Compared to the latter systems, Mg$P_2$ is unstable both thermodynamically and kinetically.

**Table 1.** Computed Natural Bond Orbital (NBO) Point Charges, Orbital Occupancies, and Wiberg Bond Indices for the Groups 2 and 12 Metals in Their Lowest Energy MP2 Complexes

| | | orbital occupancies at M | | | |
|---|---|---|---|---|---|
| M$P_2$ | $q_{\text{M}}/e$ | $n$s | ($n$ − 1)d | $n$p | WBI[a] |
| M = Be ($\eta^1$,$\eta^3$) | 1.21 | 0.24 | | 0.51 | 1.42 |
| M = Mg[b] ($\eta^6$,$\eta^6$) | 1.44 | 0.12 | 0.01 | 0.28 | 1.06 |
| M = Ca[c] ($\eta^6$,$\eta^6$) | 1.23 | 0.00 | 0.24 | 0.14 | 1.51 |
| M = Sr[d] ($\eta^6$,$\eta^6$) | 1.39 | 0.05 | 0.35 | 0.09 | 1.21 |
| M = Ba[e] ($\eta^6$,$\eta^6$) | 1.38 | 0.00 | 0.27 | 0.08 | 1.17 |
| M = Zn ($\eta^1$,$\eta^1$) | 1.08 | 0.85 | 9.95 | 0.10 | 1.22 |
| M = Cd ($\eta^1$,$\eta^1$) | 0.96 | 1.02 | 9.93 | 0.08 | 1.22 |
| M = Hg ($\eta^1$,$\eta^1$) | 0.76 | 1.30 | 9.86 | 0.07 | 1.17 |

[a] Wiberg Bond Index. [b] Some involvement, (0.16$e$) in total, of the 3d, 4p, 5p orbitals. [c] 0.4$e$ in higher orbitals. [d] 0.1$e$ in higher orbitals. [e] There is a slight involvement of the 4f and 7s orbitals.

The group 12 systems show an even greater sensitivity to the degree of the hybridization. The relatively large barriers (~4.0 to 4.9 eV) that we obtain if we accept a 50% p participation (sp hybridization) at Zn, Cd, and Hg all disappear when no hybridization is assumed (Supporting Information, Table S.2). As we will see later, the group 12 metals in the M$P_2$ complexes are essentially unhybridized. So, the barriers to dissociation in those systems are expected to be really very low.

We have been surprised that although the $\eta^1$,$\eta^1$ complex is a local minimum for M = Be, Zn, Cd, and Hg, the compromise $\eta^1$,$\eta^3$ isomer, quite stable in Be$P_2$, is not even a local minimum for the group 12 compounds. In the next section, we examine in detail the charge distribution in the M$P_2$ complexes, and trace the difference in structural preferences in the Be and group 12 systems back to the unavailability of group 12 metal $n$p orbitals for bonding.

**Charge Distribution in the Groups 2 and 12 Bis(phenalenyl) Complexes.** Computed NBO point charges and orbital occupancies for the metal centers in the minimum energy bis(phenalenyl) complexes of the groups 2 and 12 metals are listed in Table 1.

**Involvement of the ($n$ − 1)d and $n$p Orbitals in Bonding.** Notice that in the Be $\eta^1$,$\eta^3$ complex (Table 1), a significant fraction of the charge from the 2s orbital is transferred to the 2p orbitals. This is in line with the molecular orbital picture on the right in Figure 6, and confirms that the 2p orbital has a strong involvement in the bonding. The role of the valence 3p orbitals in the bonding in the Mg$P_2$ complex is harder to identify in the pictures (Supporting Information, Figure S.5), but shows up in the NBO analysis. Just under 15% (0.28$e$) of the (2.0$e$) electron population of the 3s orbital is promoted to 3p orbitals. The low bond index for Mg in the Mg$P_2$ (= 1.06) despite the high charge ($q_{\text{M}}$ = 1.44$e$) is consistent with a substantial delocalization of electron density from the metal into the $\pi$ system of the rings, supported by a weak directional (covalent) contribution to the bonding.

The importance of the $(n - 1)$d orbitals in the bonding of Ca, Sr, and Ba is underscored by the substantial population of those orbitals (0.24$e$ to 0.35$e$) in the M$P_2$ complexes and the almost complete depletion of the charge density in the ns orbitals (Table 1).

**$\eta^1$,$\eta^1$ vs $\eta^1$,$\eta^3$; (Non)-Involvement of *n*p Orbitals in the Bonding in Group 12 Complexes.** We searched unsuccessfully for the group 12 analogue of the distinctive Be$P_2$ minimum energy $\eta^1$,$\eta^3$ complex. Direct structural optimization of this $\eta^1$,$\eta^3$ isomer, (using the group 12 analogues of the Be $\eta^1$,$\eta^3$ complex (Figure 6) as our starting structures), turned up essentially the same $\eta^1$,$\eta^1$ systems shown in Figure 12 (and Supporting Information, Figure S.8). A question we ask is "Why is the $\eta^1$,$\eta^1$ structure stable for Be$P_2$ and the groups 12 complexes, but the $\eta^1$,$\eta^3$ isomer is not even a local minimum for the group 12 complexes?".

To answer this question we get some insights from a geometrically simpler series of group 12 molecules: the binary dihalides. In a recent article,[36] one of the authors and co-workers pointed out that although the lighter group 2 metals (Be and Mg) and all the group 12 metals show a strong preference for forming linear binary dihalides, *a unique characteristic of the bonding in the group 12 dihalides is the relatively poor participation of the valence p orbitals in the bonding*. This observation for the group 12 metals supports implicitly the perspective emphasized most recently by Weinhold and Landis[60] that unfilled *n*p orbitals do not play an important role in the bonding of transition (or, more generally, d-block) metals. Our NBO analysis of the group 12 bis(phenalenyl) complexes supports that view of the bonding in group 12 metals, as well. In Table 1, the *n*p orbital occupancies never rise above a paltry 0.10$e$.

The non-involvement of the *n*p orbitals in the bonding, and the low charge transfer ($q_M$) out of the *n*s orbitals for the group 12 metals (Table 1), are explained by the preferential stabilization of the *n*s orbitals by the so-called d-orbital, and lanthanide contractions, and, for Hg in particular, relativistic effects (see ref 36 and references therein). Table 2 shows a breakdown of the percentage involvement of the metal orbital versus the carbon orbital in the M—C bond in the group 12 $\eta^1$,$\eta^1$ complexes. We include, as well, the (% s, p, and d) composition for the *metal hybrid orbital* involved in the M—C bond.

Notice that the s orbitals of the metal become slightly less involved in the bonding going down group 12, especially for Hg. At the same time, the d orbitals become increasingly involved in the bonding, with a roughly 14.6% contribution to the Hg hybrid orbital. The p orbitals hardly play any role in the bonding of the group 12 complexes. These observations are in qualitiative agreement with the representation of the HOMO on the left in Figure 12, which is built up primarily of the $p_z$ orbitals on the two carbon atoms, with little reciprocation from the metal $p_z$ orbital. The HOMO-1, however, (Figure 12) has a substantial contribution from the metal *n*s orbital, which is obvious in the picture on the right in Figure 12 as a bulge in the molecular orbital in the region of the metal. Indeed, the linear C—M—C unit in the group 12 complexes may be described justifiably as a three center electron rich system in which the metal bonds predominantly through its *n*s orbital to $p_z$ orbitals of the two carbon atoms.

**Table 2.** Hybrid Orbital Composition Data for the Bis(phenalenyl)group 12 Complexes Obtained from a Natural Bond Orbital (NBO) Analysis

| | | | M hybrid orbital composition | | |
|---|---|---|---|---|---|
| M | % M | % C | s | d | p |
| M = Zn | 28.8% | 71.2% | 94.1% | 3.7% | 2.2% |
| M = Cd | 35.8% | 64.2% | 93.1% | 5.5% | 1.3% |
| M = Hg | 46.1% | 53.9% | 84.7% | 14.6% | 0.7% |

**Summary.** The non-involvement of the p orbital in the bonding of the group 12 metals makes the formation of an $\eta^3$ type bond similar to that in Be$P_2$ in Figure 7 highly unlikely for the Zn$P_2$, Cd$P_2$, and Hg$P_2$ molecules. The unavailability of the metal *n*p orbitals to support the *n*s orbital in the bonding in the $\eta^1$,$\eta^1$ complexes explains, as well, the exceptional thermodynamic instability of the group 12 complexes (Figure 13).

**Groups 2 and 12 M$P_2$ Complexes: Structural Extremes at the Ends of a Continuum.** We wondered how and why the bent $\eta^6$,$\eta^6$ sandwich complexes of the heavier group 2 metals *evolved* into the $\eta^1$,$\eta^1$ complexes when we cross the d-block and get to the group 12 metals. To satisfy our curiosity, and to better understand the influence of d-orbital occupancy on bonding, we examined the structural preferences in neutral M$P_2$ complexes of transition metals between Ca and Zn. The +2 oxidation state is common for all the period 4 transition metals except Sc and Ti. So we restricted our investigation to the neutral ($M^{2+}P^{-}{}_2$) complexes of the transition metals from V through to Cu. For each metal, we considered various $M^{2+}$ spin multiplicities (as listed in ref 61). Starting from a value of 1 or 2, we increased the multiplicity until the computed energies started to increase or until all the valence electrons were unpaired.

To be sure, state of the art multireference methods are ideal for treating transition metals, but they are very expensive. Using the B3LYP hybrid density functional, we carried out a theoretical search for the possible minimum energy structures for the individual (single reference) electron configurations for the different multiplicities of the transition metal complexes. For each optimization, our starting structure was the $\eta^6$,$\eta^6$ Ca$P_2$-type sandwich complex (Figure 11). The preferred (lowest energy) structures we obtained and the corresponding multiplicities are shown in Supporting Information, Figure S.9. Representative structures (for M = V, Co, and Cu) are included in Figure 14.

**d-Orbital Involvement and the Progression from $\eta^6$ to $\eta^1$.** The differences in the structural preferences in the heavier group 2 $\eta^6$,$\eta^6$ and group 12 $\eta^1$,$\eta^1$ complexes show the spectacular consequences of d-orbital occupation on bonding at metal centers.[19,20a,21,36]

---

(60) Weinhold, F.; Landis, C. *Valence and Bonding: A Natural Bond Orbital Donor-Acceptor Perspective*; Cambridge Univ. Press: Cambridge, U. K., 2005. For discussions on the (ir)relevance of metal np orbitals in bonding, see pp 81−82, 447−450, 477−478, and 570−573.

(61) The multiplicities considered for the transition metal complexes are ($V^{2+}$: 2, 4; $Cr^{2+}$: 1, 3, 5; $Mn^{2+}$: 2, 4, 6; $Fe^{2+}$: 1, 3, 5; $Co^{2+}$: 2, 4; $Ni^{2+}$: 1, 3; $Cu^{2+}$: 2; $Zn^{2+}$: 1).

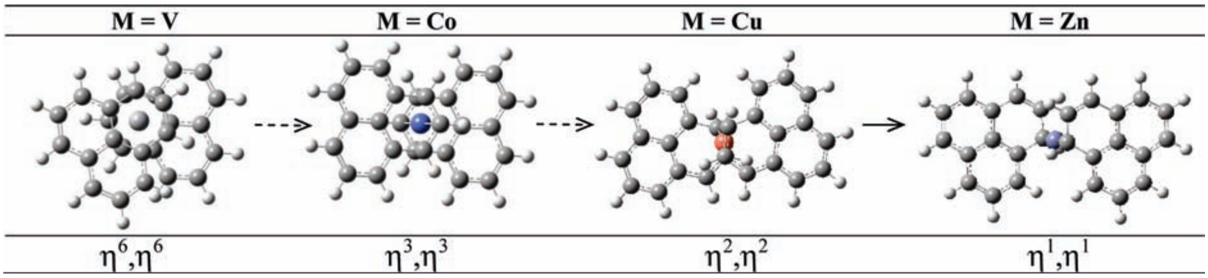

**Figure 14.** Top view of representative d-block M$P_2$ complexes showing changes in the hapticities in the lowest energy structures going across period 4: $\eta^6,\eta^6$ for M = V; $\eta^3,\eta^3$ for M = Cr, Mn, Fe, Co, and Ni; $\eta^2,\eta^2$ for M = Cu and $\eta^1,\eta^1$ for M = Zn.

A survey of the structural preferences in the lowest energy transition metal bis(phenalenyl) complexes uncovers an interesting variation in the bonding going from M = V to M = Cu. We obtain a Ca$P_2$-type $\eta^6,\eta^6$ structure for V$P_2$,$\eta^3,\eta^3$ slip sandwich structures for M = Cr, Mn, Fe, Co and Ni and an exceptional $\eta^2,\eta^2$ complex for Cu$P_2$ (Figure 14, Supporting Information, Figure S.9). For multiplicities other than those given in Supporting Information, Figure S.9 for each metal, structural optimization of the M$P_2$ complex either failed to converge or converged to a higher energy $\eta^6,\eta^6$ or $\eta^3,\eta^3$ structure.[62]

How to explain the progression in the bonding from the high hapticity vanadium complex to the low hapticity copper and zinc complexes? The involvement of the diffuse 3d-orbitals in the bonding of the early transition metals (as in the Ca, Sr, and Ba complexes) helps us to rationalize the preference for higher hapticities in their bis(phenalenyl) complexes. Going across period 4 between Ca to Zn, however, (i) the number of d orbitals available for $\sigma$ bonding decreases continuously (as more electrons are added), and (ii) the covalent radius of the metals decreases continuously (at least up to Ni; Supporting Information, Table S.3).[63,64]

The move to an $\eta^3,\eta^3$ structure after vanadium (i) allows for an optimization of the M—$P$ interactions by improving the overlap between the metal and the available (unfilled) d orbitals, and (ii) helps, as well, to minimize $P$—$P$ repulsion, which increases as the metal radius gets smaller. At copper, the opportunities for d orbital involvement are greatly diminished; hence, the preference for an even lower ($\eta^2,\eta^2$) hapticity in the Cu complex. M = Zn is the extreme case where the 3d-orbitals are unavailable for covalent bonding, and, as we showed in previous sections (see Table 2), the *n*p *orbitals are too high up in energy to be important in the bonding*.

**Transition Metal M$P_2$ Complexes: a Brief Assessment.** The molecular orbitals of the vanadium complex, are nearly identical to those of the Ca complex (see Figure 11 and the HOMO and HOMO-1 for V$P_2$ in Supporting Information, Figure S.10).

For the $\eta^3,\eta^3$ complexes obtained for M = Cr, Mn, Fe, Co, and Ni,[62] the molecular orbitals are quite similar to each other (Supporting Information, Figure S.10). One of the most important M—$P$ orbital interactions reminds us of the Be—allyl type interaction depicted in Figure 7. In all the $\eta^3,\eta^3$ transition metal complexes, three-carbon "allyl" fragments on each of the phenalenyl rings (Figure 15) interact with the transition metal d orbitals in a locally square planar environment (Figures 15; see the HOMO-1 in Supporting Information, Figures S.10, S.11).

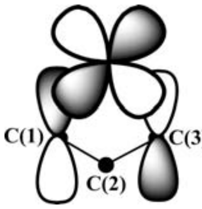

**Figure 15.** Simple representation of an important M—$P$ interaction in the transition metal $\eta^3,\eta^3$ complex (compare with the HOMO-1 in Supporting Information, Figure S.11).

**$\eta^2,\eta^2$ Copper Complex.** The $\eta^1,\eta^1$-type complex preferred by Zn$P_2$ is only a transition structure on the Cu$P_2$ potential energy surface. Structural optimizations from different starting geometries (the $\eta^6,\eta^6$, and the $\eta^3,\eta^3$ structure) all converge to the unusual $\eta^2,\eta^2$ isomer (Figure 14).

The $\eta^2,\eta^2$ Cu$P_2$ complex is a fascinating way point between the Ni ($\eta^3,\eta^3$) and Zn ($\eta^1,\eta^1$) structures. A discussion of the orbital interactions stabilizing this exceptional $\eta^2,\eta^2$ structure is included in the Supporting Information.

**Stability of the Transition Metal M$P_2$ Complexes.** BSSE corrected enthalpy changes for the formation of the most stable transition metal complexes (Supporting Information, Figure S.9) from the phenalenyl radicals and the metal atoms in their electronic ground states are summarized in Figure 16 (and are listed in Supporting Information, Table S.1).

Despite the general preferences for the $\eta^3,\eta^3$ geometry among the transition metal complexes, the binding enthalpies vary widely going across the period. The binding enthalpy is an order larger for Ni$P_2$, for instance, ($\Delta H = -2.63$ eV) than it is for Mn$P_2$ ($\Delta H = -0.25$ eV). The latter complex is the least stable of all the transition metal systems in Figure 16. Going from Ni to Cu, the decrease in the hapticity is accompanied by a dramatic decline in $\Delta H$ ($= -0.86$ eV for Cu). This small (but still negative) binding enthalpy and lower ($\eta^2,\eta^2$) hapticity for Cu$P_2$ heralds an equally precipitous change in $\Delta H$ (to $+0.94$ eV) and a further decrease in the hapticity (to $\eta^1,\eta^1$) for M = Zn. We include the data for the zinc complex in Figure 16 for comparison.

The Vanadium $\eta^6,\eta^6$ ($\Delta H = -2.78$ eV) and the Nickel $\eta^3,\eta^3$ ($\Delta H = -2.63$ eV) species (see Supporting

---

[62] See refs S.7 and S.8 in the Supporting Information.

[63] Emsley, J. *The Elements*, 3rd ed.; Oxford University Press: New York, 1998.

[64] Pyykkö, P.; Atsumi, M. *Chem.—Eur. J.* **2009**, *15*, 186.

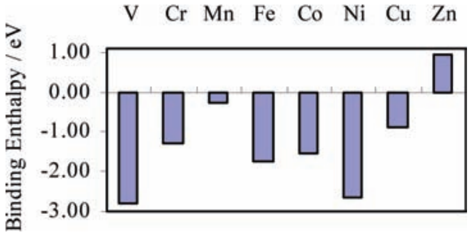

**Figure 16.** BSSE corrected binding enthalpies for the lowest energy bis (phenalenyl) transition metal complexes. The computed binding energies and enthalpies are listed in Supporting Information, Table S.1.

Information, Figure S.9) are particularly stable thermodynamically, and are expected to be the most accessible transition metal bis(phenalenyl) targets for synthesis at ambient conditions.

## Summary and Outlook

The phenalenyl radical is amazingly versatile. Because of its size, the formation of $C_{3v}$ half sandwich or high symmetry $MP_2$ sandwich structures will likely prove impossible. Nevertheless, the radical reacts (as a one electron acceptor) to form groups 2 and 12 slip sandwich structures with diverse hapticities. We find that the nature of the bonding of the phenalenyl radical and the stability of the $MP_2$ complex is extremely sensitive to the shell structure of the metals. Even among the metals in group 2, the bonding preferences differ greatly: $BeP_2$ prefers a $\eta^1$,$\eta^3$ geometry, $MgP_2$ is a weakly bound ($\eta^6$-type) sandwich complex, and the others, ($CaP_2$, $SrP_2$, and $BaP_2$), all prefer a bent $\eta^6$,$\eta^6$ sandwich structure.

The group 12 complexes form lovely $\eta^1$,$\eta^1$ slip sandwich structures; but they are unbound. A beryllium $\eta^1$,$\eta^1$ complex has been obtained, as well, but it is higher in energy than the $\eta^1$,$\eta^3$ isomer. The latter ($\eta^1$,$\eta^3$) structure that is favored by the beryllium complex is impractical for the group 12 metals owing to the unavailability (relatively high energy) of the *n*p orbitals in group 12 metals compared to the *n*s orbital. The significant stabilization of the *n*s orbitals relative to the *n*p orbitals is explained by the d-orbital and lanthanide contractions and relativistic effects in heavy atoms.[36]

Going across period 4 from the sandwich structure for M = Ca to the slip sandwich structure for M = Zn, the structural preferences of the $MP_2$ complexes change in stages. We uncover a surprising ($\eta^3$,$\eta^3$) minimum energy structure for most of the transition metal bis(phenalenyl) complexes. The hapticity in the complexes falls to from $\eta^3$ to $\eta^2$ at copper. The latter structure collapses to the unstable $\eta^1$,$\eta^1$ slip sandwich structure when we substitute for M = Zn, where the 3d subshell is completely filled.

The most thermodynamically stable of all the complexes we have studied are the Be $\eta^1$,$\eta^3$, the bent Ca, Sr, and Ba $\eta^6$,$\eta^6$, and the transition metal structures. Our results indicate that this structurally diverse set of bis(phenalenyl) complexes are strong candidates for experimental realization.

**Acknowledgment.** This research was supported by awards from Research Corporation (Cottrell College Science Award no. 7742) and from the Thomas F. and Kate Miller Jeffress Memorial Trust (Award J-903). We thank the University of Richmond and the Department of Chemistry for the award of a Puryear-Topham research fellowship to S.C., and the University of Richmond Arts and Sciences faculty research committee for supporting our work. This project emerged out of ideas formulated while K.J.D. was a postdoctoral research associate with Roald Hoffmann at Cornell University. The National Science Foundation (Grant CHE-0613306) is acknowledged for supporting the research in the Hoffmann group. Roald Hoffmann, Carol Parish, and Lawrence Scott are thanked for helpful discussions and for reading early drafts of the manuscript. We thank Gernot Frenking, László von Szentpály, and one of the reviewers for references.

**Supporting Information Available:** Additional information as noted in the text. This material is available free of charge via the Internet at http://pubs.acs.org.